Impact of the Uncertainty of Distributed Renewable Generation on Deregulated Electricity Supply Chain

Hanling Yi, Mohammad H. Hajiesmaili, Ying Zhang,
Minghua Chen, *Senior Member, IEEE*, Xiaojun Lin, *Fellow, IEEE*

***Abstract*—Active districts are districts that have a system in place to coordinate distributed energy generation and external grid to meet the local energy demand. They are now widely recognized as a clear opportunity towards distributed renewable integration. Despite apparent benefits of incorporating renewable sources in an active district, uncertainty in renewable generation can impose unprecedented challenges in efficient operation of the existing deregulated electricity supply chain, which is designed to operate with no or little uncertainty in both supply and demand. While most previous studies focused on the impact of renewables on the supply side of the supply chain, we investigate the impact of distributed renewable generation on the demand side. In particular, we study how the uncertainty from distributed renewable generation in an active district affects the average buying cost of utilities and the cost-saving of the active district. Our analysis shows that the renewable uncertainty in an active district can (i) increase the average buying cost of the utility serving the active district, termed as *local impact*, and (ii) somewhat surprisingly, reduce the average buying cost of other utilities participating in the same electricity market, termed as *global impact*. Moreover, the local impact will lead to an increase in the electricity retail price of active district, resulting in a cost-saving less than the case without renewable uncertainty. These observations reveal an inherent economic incentive for utilities to improve their load forecasting accuracy, in order to avoid economy loss and even extract economic benefit in the electricity market. We verify our theoretical results by extensive experiments using real-world traces. Our experimental results show that a 9% increase in load forecasting error (modeled by the standard deviation of the mismatch between real-time actual demand and day-ahead purchased supply) will increase the average buying cost of the utility by 10%.**

***Index Terms*—Active District, Electricity Market, Distributed Renewable Generation, Electricity Price.**

I. Introduction

Renewable energy sources, including solar PVs and wind turbines, are effective means to de-carbonize the power system and support sustainable economic and social development. In 2014, renewables represented approximately 58.5% of net additions to global power capacity, enough to supply around 7.6% of global electricity if operated at $1/3$ of the installation capacity [20].

The work presented in this paper was supported in part by National Basic Research Program of China (Project No. 2013CB336700), and the University Grants Committee of the Hong Kong Special Administrative Region, China (Theme-based Research Scheme Project No. T23-407/13-N and Collaborative Research Fund No. C7036-15G), and National Science Foundation through grants CCF-1442726 and ECCS-1509536.

Hanling Yi, Mohammad H. Hajiesmaili, Ying Zhang, and Minghua Chen are with Department of Information Engineering, the Chinese University of Hong Kong. Xiaojun Lin is with School of Electrical and Computer Engineering, Purdue University.

A popular platform for incorporating renewable energy sources is active district. An active district is a local electric power system typically resided in low-voltage distribution network, consisting of various distributed generation, storage systems, and responsive load. In an active district, all the distributed generation resources are owned by the same entity, and it can coordinate local generation and the external grid to meet the energy demand of a local community, such as a university campus or a hospital. Active districts can be regarded as microgrids operating in grid-connected mode, which are more robust and cost-effective than conventional approach of centralized grids and represent a promising paradigm of future power system [15].

Our study focuses on active districts with non-dispatchable, intermittent, and unpredictable renewables energy, such as wind and solar. The intermittent renewable generation not only introduces unprecedented challenges to active district operation, for example energy generation scheduling [11], [14], [25], but also may lead to nontrivial impact on electricity procurement of utilities on a regional market, as we show in this paper. In the deregulated electricity supply chain illustrated in Fig. 1, an active district (or a microgrid) obtains electricity from a local utility to serve its residual demand after deducting its actual demand by renewable generation. The local utility, serving as a retailer, obtains electricity supply from the regional electricity market to serve a group of customers. The regional market operator (governed by an independent system operator) provides a trading place, determines a market clearing price based on the supply offers and demand bids using a double-sided auction mechanism, and matches the supply and demand at the price. The market operates in a *two-settlement* manner and settles transactions at two different timescales and prices, i.e., one day ahead with day-ahead price and real-time with spot price. In day-ahead market operation, the generation companies (respectively utilities) submit their offers (respectively bids) for selling (respectively buying) electricity for the next day, based on generation (respectively load) forecasting. Then, the imbalance between day-ahead procurement and actual load is settled in real-time market operation. We refer to Sec. II-B for more details about the two-settlement market.

Active district with renewable source can impose challenges in electricity market operations due to the intermittent and unpredictable nature of renewable generation. Our goal is to investigate the impact of the renewable uncertainty on the *average buying cost* per unit electricity (ABC) of utilities (formally defined in Sec. II-C). We note that most of the

previous studies focus on the impact of renewables on the *supply side* of the supply chain where the renewables, such as large wind farms, participate in deregulated markets as generation companies [6], [17], [21], [26]. In contrast, our study, along with a few others [8], [12], [16], investigates the impact of renewables on the *demand side*, where the distributed renewable generation affect the residual demand to be fulfilled by the supply chain. For instance, McConnell *et al.* show that distributed solar generation can reduce the electricity demand and depress the wholesale price, which also known as the merit-order effect [16]. However, the reduction in local demand due to renewable generation may force the utilities to raise the retail electricity price in order to recover their capital cost in transmission and distribution infrastructure [8]. As a result, retail customers with distributed renewable generation may observe less cost-saving than expected. In this paper, we investigate the impact of uncertainty from distributed renewable generation on the electricity supply chain.

In particular, we aim to answer two fundamental questions:

- What is the *local impact* of distributed renewable uncertainty? Namely, how does renewable uncertainty in an active district affect the ABC of the utility serving the active district?
- What is the *global impact* of distributed renewable uncertainty? Namely, how does renewable uncertainty in an active district affect the ABCs of all other utilities participating in the same regional market?

Answers to the above questions provide a complete understanding of the impact of distributed renewable generation on the economic operation of all the utilities participating in the regional market. We carry out a comprehensive study and make the following contributions.

▷ We show that the utility with larger renewable penetration will suffer from higher ABC. This answers the first question on the local impact of distributed renewable uncertainty. The increase in ABC will lead to an increase in the electricity retail price of the active district. As a result, an active district with renewable generation uncertainty observes less cost-saving than the case without generation uncertainty.

▷ Somewhat surprisingly, we show that all other utilities participating in the same regional market will actually observe a decrease in their ABCs. This answers the second question on the global impact of distributed renewable uncertainty. The observations reveal an inherent economic incentive for utilities to improve their load forecasting accuracy, in order to avoid losses and even extract economic benefit.

▷ We characterize a set of sufficient conditions for observing the above-mentioned local and global impacts. These conditions, on load forecasting errors and the relationship between day-ahead prices and real-time prices, suggest that the above-mentioned local and global impacts can be observed under rather general settings, for example when load forecasting errors follow arbitrary symmetric distribution with zero mean.

▷ We verify our theoretical results by extensive real-world trace-driven experiments with different percentages of renewable penetration. In a set of representative experiments, our results demonstrate that a 9% increase in load forecast error will increase the ABC of the utility by 10%. Our experiments also validate that the active district with renewable generation uncertainty observes less cost-saving than the case without generation uncertainty.

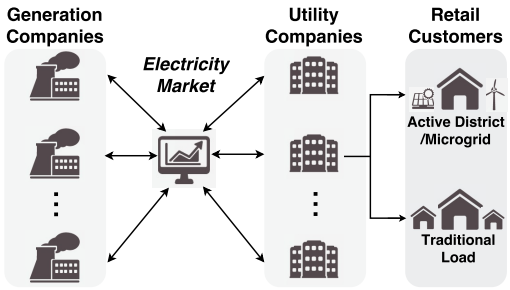

Fig. 1. The deregulated electricity supply chain

The rest of this paper is organized as follows. Sec. II gives a brief introduction on deregulated electricity supply chain and its pricing model. Our theoretical results are presented in Sec. III. Experimental results are included in Sec. IV. Sec. V concludes the paper.

Due to space limitation, all the proofs are in our technical report [24], unless otherwise specified.

II. Deregulated Electricity Supply Chain

In what follows we explain the electricity supply chain, the operation of the electricity market, and the market pricing model.

A. Electricity Supply Chain

As illustrated in Fig. 1, the deregulated electricity supply chain consists of the following four components [13]:

- Retail customers (in particular, active districts or microgrids), the end-users that consume electricity.
- Utilities, who submit bids to buy electricity supply in the market in order to serve a group of retail customers.
- Generation companies, i.e., power plant owners who produce electricity and submit offers to sell electricity in the market.
- Electricity market, administered by an independent system operator (e.g., ISO-NE [1]), that provides a trading place, matches supply offers from generation companies and demand bids from utilities.

Utilities transact electricity with generation companies in the wholesale electricity market, and the active district and traditional load (residential or commercial load) procure electricity from the local utility. In addition, distributed renewable generation is incorporated by some of the retail customers (active districts or microgrids) to satisfy part of their demand locally.

B. Electricity Market Model

The electricity market usually operates in a *two-settlement* manner and settles transactions at two different timescales and prices, i.e., day ahead with day-ahead price and real-time with spot price.

Day-Ahead Market Operation. In the day-ahead market operation, generation companies and utilities submit their

offers and bids for selling and buying the electricity for each hour of the next day, based on generation and load forecasting. The market operator then clears the market and determines the day-ahead price through a double-sided auction mechanism. The day-ahead market operation allows generation companies to schedule their supply one day before actual dispatch, in order to enhance reliability and improve efficiency of the unit commitment decision. According to a report from the NYISO market, about 90% of the electricity supply is scheduled in the day-ahead market operation [3].

Real-Time Market Operation. The real-time market is dedicated to balancing the supply and demand in real-time operation. The transactions for the utilities and generation companies in real-time market operation are settled on a hourly basis. In Nord Pool [2], for example, the ISO collects offers from generation companies and determines the hourly real-time spot price based on the actual supply and demand. When the supply is less (respectively higher) than the demand, the market is up-regulated (respectively down-regulated) and the real-time spot price is larger (respectively smaller) than the day-ahead price [10]. Overall, the real-time market operation settles the imbalance between the day-ahead scheduled amounts of electricity and the real-time actual demand.

C. Electricity Pricing Model

In our model, we assume that N utilities, indexed by i, participate in the electricity market. Without loss of generality, we focus on the settlements of electricity supply of a particular hour. We denote the corresponding day-ahead price and the spot price as p_d and p_s (unit: \$/MWh), respectively. In this paper, we assume that the day-ahead price is given and is not affected by utility i's day-ahead purchased amount. This assumption is reasonable since the majority of the electricity is traded in the day-ahead market and a single utility does not have the market power to manipulate the market price. The spot price is related to both the day-ahead price and aggregate mismatch to be balanced on the real-time market, which will be discussed more later in this section.

Average Buying Cost per Unit Electricity Of Utility. Define D_i (unit: MWh) as the real-time actual demand of utility i at the particular hour. Further, denote Δ_i (unit: MWh) as the mismatch between the real-time actual demand and day-ahead purchased supply for utility i in the real-time market operation. Then the day-ahead purchased supply for utility i in the day-ahead market operation is $D_i - \Delta_i$. Whenever there is an imbalance, i.e., $\Delta_i \neq 0$, the utility has to settle this imbalance in the real-time market operation at the spot price p_s, i.e., it either sells the residual electricity back to the market when $\Delta_i < 0$, or buys the deficient electricity from the market when $\Delta_i > 0$. In this way, the total electricity cost of utility i in the market, denoted as C_i, is defined as follows (unit: \$):

$$C_i \triangleq p_d(D_i - \Delta_i) + p_s\Delta_i. \tag{1}$$

In other words, for utility i, its actual demand D_i is settled in two timescales: (i) an amount of $D_i - \Delta_i$ is settled in day-ahead operation at price p_d, and (ii) the remaining amount Δ_i is settled in real-time operation at the spot price p_s. Given the actual electricity delivery D_i, we now define the Average Buying Cost per unit electricity (ABC) for utility i as

$$\begin{aligned} \mathsf{ABC}_i &\triangleq \frac{C_i}{D_i} \\ &= \frac{1}{D_i}\left[p_d\left(D_i - \Delta_i\right) + p_s\Delta_i\right], \end{aligned} \tag{2}$$

whose unit is \$/MWh. If utility i has an accurate prediction for D_i in the day-ahead market operation, i.e., $\Delta_i = 0$, then its ABC_i is simply the day-ahead price p_d. In practice, it is common that $\Delta_i \neq 0$ due to load forecasting error, because of for example renewable uncertainty. The ABC_i in this case depends on the real-time spot price too.

Real-time Spot Price. The spot price is in general affected by the real-time market imbalance, i.e., the day-ahead scheduled supply and the real-time actual demand. Any displacement in the market imbalance will cause the spot price to deviate from the day-ahead price. Specifically, deficient supply in the market leads to a higher spot price, while excessive supply results in a lower spot price. To capture their relationship, we first denote the aggregate imbalance from all the utilities in real-time market operation as $\Delta \triangleq \sum_{i=1}^{N}\Delta_i$, and consider first the following model for real-time spot price [18][1]:

$$p_s = \begin{cases} p_d, & \Delta = 0, \\ (b_1 + a_1\Delta)p_d, & \Delta > 0, \\ (b_2 + a_2\Delta)p_d, & \Delta < 0. \end{cases} \tag{3}$$

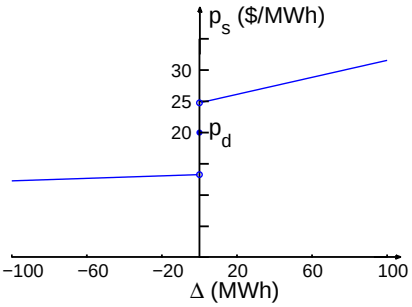

Fig. 2. The model of real-time spot price p_s as a function of day-ahead price p_d and aggregate real-time imbalance Δ.

Remark: (i) The model[2] was proposed in [18] by curve-fitting historical data. In particular, [18] suggests that $a_1 = 0.0034, a_2 = 0.0005$, $b_1 = 1.2378$, and $b_2 = 0.6638$. The corresponding function is shown in Fig. 2 with $p_d = 20$. (ii) The spot price function is discontinuous at $\Delta = 0$, i.e., $b_1 > 1 > b_2$. This discontinuity can be interpreted as a *premium of readiness* that utilities need to pay for the generation companies, since they have to generate urgent regulating power upon notice [22]. (iii) In this paper, we

[1]In practice the spot price also depends on generation imbalance, i.e., in the event of generator trips or as a result of large-scale renewable generation. This generation imbalance can increase the variability of the market imbalance. We note that this paper mainly focuses on the demand side of the electricity supply chain and we do not consider the effect of generation uncertainty on the market imbalance. This simplification will reduce the variance of market imbalance.

[2]In general, a_1, a_2, b_1, b_2 should be positive.

mainly work with the pricing model in (3), to bring out the insights clearly. However, our insights are not restricted to the model in (3). In Section III-C, we will show that the local and global impacts hold for a larger class of pricing models, which may be non-linear and/or continuous at $\Delta = 0$.

III. Impact of Uncertainty of Distributed Renewable Generation on ABCs

Recall that Δ_i is the mismatch between the actual load served by utility i during the real-time market operation and the electricity purchased by utility i from the day-ahead market operation. We assume that each Δ_i is a Gaussian random variable with mean zero and variance σ_i^2, i.e.,

$$\Delta_i \sim \mathcal{N}(0, \sigma_i^2), \quad i = 1, 2, ..., N,$$

and they are mutually independent. Here, the variance σ_i^2 reflects the load forecasting accuracy; a large value of σ_i^2 indicates a (statistically) large forecasting error. As an active district served by utility i incorporates more renewable generation, utility i observes a residual demand of active district that is smaller in volume but more difficult to predict accurately. More specifically, uncertainty in renewable generation is inherited by the residual demand of active district. It is thus difficult for utility i to accurately predict its load, resulting in a large load forecasting error and thus a large σ_i^2. We remark that the Gaussian distribution is commonly adopted to model load forecasting error [7], [17], [19], [23]. Our analysis extends to any forecasting errors that follow a symmetric distribution with zero mean, as discussed in Sec. III-C.

Recall that $\Delta = \sum_{i=1}^{N} \Delta_i$ is the total imbalance in the real-time market operation. For ease of discussion, we define

$$\Delta_{-i} \triangleq \Delta - \Delta_i = \sum_{j:j\neq i}^{N} \Delta_j, \tag{4}$$

as the aggregate mismatch of all other utilities except utility i. It is straightforward to verify that Δ_{-i} is a random variable with mean zero and variance

$$\sigma_{-i}^2 = \sum_{j:j\neq i}^{N} \sigma_j^2, \tag{5}$$

where σ_{-i}^2 represents the aggregate forecasting errors of all utilities except utility i. Here we assume that the load forecasting errors are mutually independent. This assumption allows us to obtain analytically tractable result and helps us gain valuable insights. However, in practice the load forecasting errors may not be independent, as we demonstrated in the experiment in Sec. IV. We still observe local and global impact, as suggested by the analysis, which depicts the robustness of our main results w.r.t. the correlations in load forecasting errors.

Next, we will first characterize the expected ABCs of utilities as a function of load forecasting error, represented by σ_i^2 and σ_{-i}^2. We will then discuss the results and insights.

Theorem 1. *Under the model of (3), the expectation of* ABC_i *is given as:*

$$\begin{aligned}\mathbb{E}\left[\mathsf{ABC}_i\right] =& \mathbb{E}\left[\frac{1}{D_i}\left[p_d\left(D_i - \Delta_i\right) + p_s\Delta_i\right]\right] \\ =& p_d + \frac{(a_1+a_2)p_d}{2D_i}\sigma_i^2 \\ &+ \frac{(b_1-b_2)p_d}{2D_i}\mathbb{E}\left[\Delta_i \cdot \mathrm{erf}\left(\frac{\Delta_i}{\sqrt{2}\sigma_{-i}}\right)\right], \end{aligned} \tag{6}$$

where $\mathrm{erf}(x) = \frac{1}{\sqrt{\pi}}\int_{-x}^{x} e^{-t^2}dt$ *is the standard error function, and coefficients* a_1*,* a_2*,* b_1*, and* b_2 *are parameters of the pricing model defined in* (3)*.*

Remarks: The expected ABC_i in (6) depends on three terms. The first term is simply the day-ahead market clearing price. The second and the third terms correspond to utility i's cost for balancing its mismatch in the real-time market operation. Here, the second term is affected by utility i's load forecasting accuracy. The third term, interestingly, is affected by not only the forecasting accuracy of utility i, but also the aggregate forecasting accuracy of all other utilities. Thus, the close-form expression of $\mathbb{E}\left[\mathsf{ABC}_i\right]$ allows us to investigate how the change in one utility's forecasting accuracy affects its own expected ABC, i.e., local impact, as well as those of all other utilities participating in the same regional market, i.e., global impact.

For ease of discussion on local and global impacts, we present the following understanding. Recall that the distribution of Δ_i is symmetric. By the Total Expectation Theorem, we have

$$\mathbb{E}\left[\mathsf{ABC}_i\right] = \int_0^{+\infty} \phi(\delta_i, \sigma_{-i}^2) f_{\Delta_i}(\delta_i) d\delta_i, \tag{7}$$

where

$$\phi(\delta_i, \sigma_{-i}^2) \triangleq \mathbb{E}_{\Delta_{-i}}\left[\mathsf{ABC}_i | \Delta_i = \delta_i\right] + \mathbb{E}_{\Delta_{-i}}\left[\mathsf{ABC}_i | \Delta_i = -\delta_i\right],$$

represents the average buying cost per unit electricity for utility i when its mismatch is $|\delta_i|$ in volume, and $f_{\Delta_i}(\cdot)$ is the PDF of random variable Δ_i. We have the following observation on $\phi(\delta_i, \sigma_{-i}^2)$.

Lemma 1. *Given fixed* σ_{-i}^2*,* $\phi(\delta_i, \sigma_{-i}^2)$ *is increasing w.r.t.* δ_i*.*

Essentially, Lemma 1 says that the average buying cost of utility i increases as it has more mismatch (either positive or negative) to balance.

Lemma 2. *Given fixed* δ_i*,* $\phi(\delta_i, \sigma_{-i}^2)$ *is decreasing w.r.t.* σ_{-i}^2*.*

Lemma 2 says that the average buying cost of utility i to balance a fixed amount of mismatch $|\delta_i|$ will decrease if other utilities in the market have larger load forecasting errors. The details of why $\mathbb{E}[\mathsf{ABC}_i]$ is decreasing w.r.t. σ_{-i}^2 can be found in Appendix C.

The intuitions and insights are included in the proof sketches of the two lemmas in Appendixes A and B. The observations in the lemmas are useful in the discussion on the local and global impacts in the next two subsections.

A. Local Impact of Uncertainty of Distributed Renewable Generation

The local intermittent renewable generation introduces extra uncertainty in the residual demand of the active district. Consequently, the utility serving the active district (among its other customers) will observe statistically larger load forecasting error, and the regional market will need to settle (statistically) larger supply-and-demand imbalance in the real-time market operation. A careful analysis shows that the utility with larger load forecasting error will suffer from an increase in its ABC. We summarize this observation into the following corollary.

Corollary 1. *Consider utility i, given fixed σ_{-i}^2, $\mathbb{E}[\mathsf{ABC}_i]$ is monotonically increasing w.r.t. σ_i^2. Hence, if the uncertainty of distributed renewable generation deteriorates the forecasting accuracy and leads to a larger σ_i^2, then utility i will suffer from higher expected* ABC.

We explain the intuition behind Corollary 1 as follows. Recall that expected ABC of utility i can be expressed in (7), where the integral can be interpreted as weighted sum of $\phi(\delta_i, \sigma_{-i}^2)$ with different $\delta_i > 0$. When σ_i^2 increases, $\Delta_i \sim \mathcal{N}(0, \sigma_i^2)$ is more likely to take values of large magnitude, resulting in a larger weight for $\phi(\delta_i, \sigma_{-i}^2)$ with large δ_i. Now, under the setting of Corollary 1, $\phi(\delta_i, \sigma_{-i}^2)$ is increasing w.r.t. δ_i from Lemma 1, thus $\mathbb{E}[\mathsf{ABC}_i]$ increases as σ_i^2 increases.

B. Global Impact of Uncertainty of Distributed Renewable Generation

We now show that the uncertainty of distributed renewable generation in active districts not only increases the expected ABC of the utility serving the active districts, but also decreases the expected ABCs of all other utilities participating in the same market.

Corollary 2. *Consider all utilities except utility i, given fixed σ_j^2, $1 \le j \le N$ and $j \ne i$, $\mathbb{E}[\mathsf{ABC}_j]$ is monotonically decreasing w.r.t. σ_i^2. The "reverse" direction is also true: consider utility i, given fixed σ_i^2, $\mathbb{E}[\mathsf{ABC}_i]$ is monotonically decreasing w.r.t. σ_{-i}^2.*

Remark: (i) Corollary 2 implies that a utility serving customers with distributed renewable generation will "benefit" other utilities on the same market by reducing their expected ABCs, and conversely a utility serving customers without renewable uncertainty will enjoy a lower expected ABC when customers of other utilities install renewable generation. (ii) Corollaries 1 and 2 are significant in that they reveal an inherent economic incentive for utilities to improve their load forecasting accuracy, in order to avoid economy loss and even extract economic benefit when the electricity market is operating under a volatile condition.

We present the intuition for Corollary 2 as follows. It suffices to focus on the "reverse" direction, i.e., we fix σ_i^2 while increase σ_{-i}^2 to evaluate the changes in $\mathbb{E}[\mathsf{ABC}_i]$. According to (7), when σ_i^2 is fixed, the distribution of Δ_i, i.e., $f_{\Delta_i}(\delta_i)$, is fixed. From Lemma 2, we know that $\phi(\delta_i, \sigma_{-i}^2)$ is decreasing w.r.t. σ_{-i}^2 given fixed δ_i. Since each term in the integral in (7) decreases as σ_{-i}^2 increases, $\mathbb{E}[\mathsf{ABC}_i]$ decreases as well.

C. Sufficient Conditions for Observing the Local and Global Impacts

The local and global impacts reported earlier are obtained under the linear pricing model in (3). An important question to be addressed is under what condition on the pricing model and what distribution on the imbalance Δ_i, that we can observe similar types of local and global impacts? In the following, we answer the question and generalize the previous results.

Theorem 2. *Assume that for any $1 \le i \le N$, the imbalance Δ_i follows a symmetric distribution with mean zero and variance σ_i^2, and they are mutually independent. Denote the price function as $p_s = p(x)$. The following statements are true:*

(1) If $p(x)$ is increasing w.r.t. x, then for any $1 \le i \le N$, given a fixed σ_{-i}^2, $\mathbb{E}[\mathsf{ABC}_i]$ monotonically increases as σ_i^2 increases. In other words, Corollary 1 holds for any price function that is increasing w.r.t. x.

(2) If $p(x)$ is differentiable for all x except the origin, i.e., $p'(x)$ exists for all $x \in \mathbb{R} \setminus \{0\}$, and either

$$\begin{aligned} &p(0^+) = p(0^-), \\ &p'(\xi_1) + p'(-\xi_1) < p'(\xi_2) + p'(-\xi_2), \quad \forall \xi_1 > \xi_2 > 0, \end{aligned} \tag{8}$$

or

$$\begin{aligned} &p(0^+) > p(0^-), \\ &p'(\xi_1) + p'(-\xi_1) \le p'(\xi_2) + p'(-\xi_2), \quad \forall \xi_1 > \xi_2 > 0, \end{aligned} \tag{9}$$

then for any $1 \le i \le N$, given a fixed σ_i^2, $\mathbb{E}[\mathsf{ABC}_i]$ monotonically decreases as σ_{-i}^2 increases. In other words, Corollary 2 holds for any price function satisfying (8) *or* (9).

Remark: (i) Results in Corollary 1 and 2 are special cases of Theorem 2 under assumptions of Gaussian distribution for Δ_i and the pricing model in (3). In particular, the price function in (3) satisfies the condition in (9). (ii) Theorem 2 generalizes previous results to a larger class of pricing models. For example, we can observe local and global impacts under the two price functions given in Fig. 3. We note that the price function on the left is continuous at $\Delta = 0$ while the right one is discontinuous at $\Delta = 0$. (iii) This theorem applies to any Δ_i following symmetric distribution with zero mean.

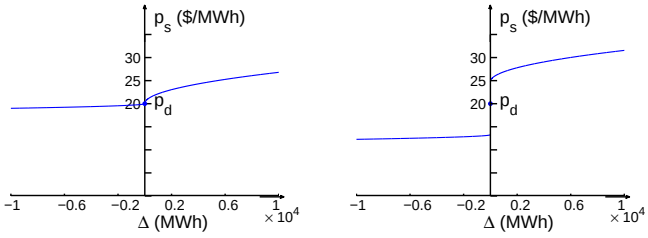

(a) $b_1 = b_2 = 1$ (b) $b_1 = 1.2378$, $b_2 = 0.6638$

Fig. 3. Nonlinear pricing function $p(x) = p_d \times (1_{\{x>0\}}(a_1 x^k + b_1) + 1_{\{x<0\}}(-a_2(-x)^k + b_2) + 1_{\{x=0\}})$ with $a_1 = 0.0034$, $a_2 = 0.0005$, $p_d = 20$, and $k = \frac{1}{2}$, where $1_{\{\cdot\}}$ is the indicator function. Note that to show the nonlinear relationship more clearly, we vary Δ from -10GWh to 10GWh.

IV. Experimental Results

A. Experiment Settings

Scenarios and Experiment Procedure. We simulate an electricity market with 10 utilities. In the electricity market,

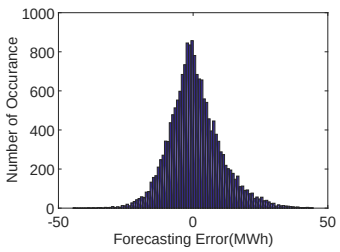

Fig. 4. The histogram of load forecasting error for a utility using ANN model.

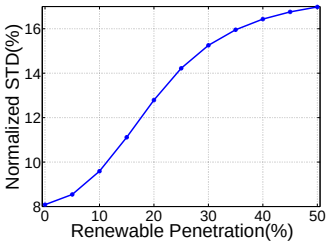

Fig. 5. The normalized standard deviation for the utility with various renewable penetration in active district.

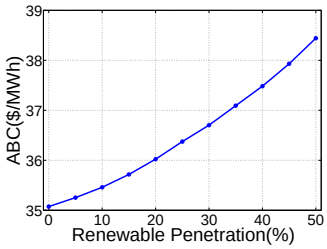

Fig. 6. The mean of ABC for the utility with various renewable penetration in active district.

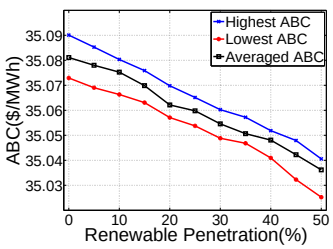

Fig. 7. The mean of ABC for other utilities with fixed renewable penetration in active district.

each utility participates in both day-ahead and real-time market operations. The spot price is obtained from the pricing model in (3) and the parameters in [18]. For each hour, the ABC is computed according to (2) and the retail price for the active district is set as the same as the ABC, following real-time pricing scheme for the retail customers. As in our experiments we aim to measure the cost-saving of the active district, we have used the total electricity cost of the active district as the metric, which is defined as the product of the retail price and residual demand.

Experimental Data. We use the hourly day-ahead price data from the PJM market to conduct the experiments [5]. The mean of the day-ahead price is 35$/MWh. The hourly electricity demands are obtained from 10 utilities in the PJM market and the electricity consumptions from these 10 utilities are scaled to have the same mean (2GWh). We incorporate renewable energy supply sources by the wind power trace from the PJM market and scale it down to obtain different levels of renewable penetration in active district. We define the renewable penetration in the active district as the ratio between average renewable generation and peak demand of active district. Unless otherwise specified, we assume the utilities have 30% of its demand coming from the active district, and the renewable penetration in active district is fixed at 10%. Meanwhile, weather information including temperature, humidity, pressure, and wind speed are gathered from the Pennsylvania State Climatologist [4] to perform load forecasting.

B. Impact of Renewable Uncertainty

Purpose: As new types of retail customers with local renewable sources in electricity supply chain, active districts exhibit large fluctuations in their net demand due to the uncertainty from renewables. Previous analysis highlights the negative impact of renewable uncertainty on the load forecasting accuracy, but it remains unclear to what extent this renewable uncertainty can affect the load forecasting accuracy. This subsection aims to answer this question.

Nowadays, various load forecasting tools have been employed to perform the day-ahead prediction. For example, similar day method, Artificial Neural Network (ANN), and regression analysis are used in ISO-NE [1]. In our experiments, we use an ANN model to conduct load forecasting, and the load forecasting errors are obtained by subtracting the forecasted demands from the true demands. Note that in the experiments, we do not preset a model for the load forecasting errors.

The artificial neural network, which is composed of a number of interconnected neurons with different connection weights, was first developed by researchers to mimic the structure of the human brain. Through a learning process based on the training data set, ANN adjusts the connection weights among neurons and generates a mapping between the inputs and the outputs. Once the ANN is trained, it can then be utilized to predict target value based on the input data. In our experiments, the training of a three-layer feedforward neural network is performed by Neural Network Toolbox in MATLAB [9] using the Levenberg-Marquardt algorithm. The target value is the load consumption, and the input data to train the ANN model include the weather information, the holiday information, the 24-hour-ahead load consumption and the 48-hour-ahead load consumption.

Observations:

We observe that the load forecasting errors in our experiments do not follow normal distribution. To see this, in Fig. 4 we plot the histogram of forecasting error for a utility. The distribution is symmetric, and the mean and standard deviation of the samples are 0.7659 and 9.7391, respectively. We then use the *Lilliefors Goodness-of-Fit Test* to perform the normality test on the load forecasting error samples. It turns out that the null hypothesis (i.e., "the data are normally distributed") is rejected at the 5% significant level. This observation demonstrates the robustness of our analysis. Namely, for our main results to hold, the load forecasting errors need not necessarily follow a normal distribution. As stated in Theorem 2, the main results extend to any forecasting errors that follow a symmetric distribution with zero mean. In addition, we note that there are correlations in the load forecasting errors among different utilities, and the largest correlation coefficient is 0.76 in the experiments.

We define the normalized standard deviation as the standard deviation of load forecasting error in all hours normalized by the mean of actual load. As shown in Fig. 5, the load forecasting error increases as the renewable penetration continues to grow in the active district. In particular, we can observe an increasing normalized standard deviation from roughly 8% under no renewable condition to around 17% when the renewable penetration reaches 50% in active district. We note that although the mean absolute percentage error (MAPE)

is commonly used as a measure of prediction accuracy of a forecasting method in statistics, here we use normalized standard deviation instead, since the variance is commonly used to model the load forecasting error in the power system literature [7], [17], [19], [23].

C. Impact of Increasing Load Forecasting Error

Purpose: As suggested in Sec. III, the increasing load forecasting error in one utility will increase the ABC of this utility and decrease the ABC of all other utilities on the same market. In this subsection, we conduct experiments to verify our theoretical results. Toward this end, we vary the renewable penetration of the active district in one utility from 0% to 50%, while fixed the renewable penetration of the active district in all other utilities and measure the ABCs. We note that each point in the following figures is the average ABC of the utility under 17520 different executions (2 years hourly data).

Observations: Fig. 6 shows the average of ABC for the utility with active district as its retail customer under different levels of renewable penetration. The result depicts that as renewable penetration increases, the ABC increases as well. Note that when the renewable penetration reaches 50% in active district, the ABC of the utility increases by more than 10% as compared to the case with no renewable penetration. This observation further verifies the result in Corollary 1 on the local impact of uncertainty in distributed renewable generation.

Fig. 7 demonstrates the decrease of the ABC for other utilities (we have plotted the results for the utilities with the highest ABC, the lowest ABC, and the average ABC of other 9 utilities to keep the figure clear). This decrease is consistent with the analysis in Sec. III, that the increasing load forecasting error in one utility can benefit other utilities by reducing their ABC. As compared to the amount of increase in the ABC of the utility with active district (10% with 50% penetration), the decrease in the ABC of the others is rather minor (0.1% decrease with 50% penetration, on average). From Fig. 5, we know that as the renewable penetration in active district increases from 0% to 50%, the load forecasting error of the utility will increase from 8% to 17%. Theoretically, we can compute from (6) that the ABC of this utility will increase by 10% and the ABC of other utilities will decrease by 0.08% under our simulation setting (Please refer to the experiment settings in Sec. IV-A, we use the mean of p_d and D_i to approximate the ABC when σ_{-i} takes two different values, and calculate its relative change in percentage). In other words, the simulation result matches the theoretical result. We note that the local impact only affects one utility, while the global impact can affect all other utilities in the electricity market. In this sense, the global impact is significant as well.

D. Implication on the Cost-saving of the Active District

Purpose: The increase in the ABC of the utility eventually leads to the increase in the retail price for customers. In this way, even though the active district increases the renewable penetration and reduces its electricity demand, it will observe less cost-saving as compared to the case without renewable uncertainty, since the increased retail prices caused by the renewable uncertainty partially offset the benefit of the renewable generation. To evaluate the impact of the renewable uncertainty on the cost-saving of active district, in this subsection, two different scenarios are considered: 1) the utility predicts the day-ahead demand with ANN prediction method; 2) the utility has accurate day-ahead demand prediction. The two scenarios differs in the utility's ability to predict the future demand. The second scenario serves as the benchmark to study the impact of renewable uncertainty.

We define the cost-saving as $\eta(x) = \frac{C_m - C(x)}{C_m}$, where C_m is the cost of active district without renewable energy and $C(x)$ is the cost of active district with different renewable penetration levels ($x \in \{5\%, 10\%, ..., 50\%\}$). We denote $\eta^{ANN}(x)$ and $\eta^{AP}(x)$ as the cost-saving with ANN prediction method and accurate prediction, respectively. Then the cost-saving reduction is formally defined as $\eta^{AP}(x) - \eta^{ANN}(x)$. Small cost-saving reduction indicates a small impact of renewable uncertainty on the cost-saving of active district.

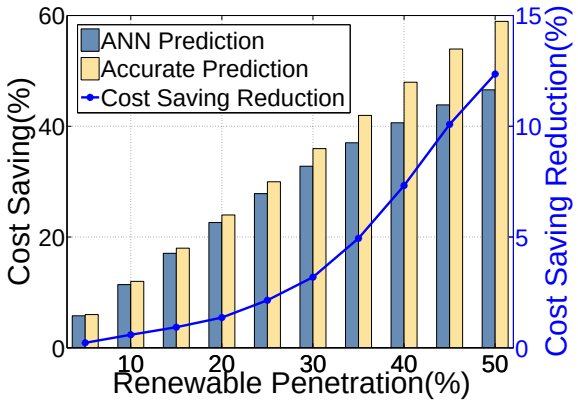

Fig. 8. The percentage of cost-saving and cost-saving reduction in active district

Observations: Results in Fig. 8 depict that the cost-saving of active district increases with high renewable penetration. This is reasonable as the renewable generation is free of charge and the more renewable generation, the less electricity active district needs to buy from the utility. However, the cost-saving reduction in active district is increasing as renewable penetration in active district increases, which demonstrates the negative impact of renewable uncertainty. The uncertainty of renewable increases the ABC of the utility and consequently the retail price, which partially offset the benefit of renewable generation in active district.

E. Impact of Increasing Renewable Penetration in Multiple Utilities

Purpose: Previous experiments have focused on the scenarios that increase of renewable penetration occurs only in one utility, while other utilities on the same market have fixed renewable penetration. In practice, multiple utilities may simultaneously suffer larger load forecasting error due to increase of renewable penetration. In this subsection, we consider the scenarios that multiple utilities have increasing renewable penetration and investigate the changes in their

ABCs[3]. More specifically, we assume that utilities in the market can be categorized into two groups, with 6 of them belong to group-1 and 4 of them belong to group-2. In this experiment, we consider two scenarios for comparison. In the first scenario, group-1 utilities have an annual increase in renewable penetration at 5%, while group-2 utilities have an annual increase at 10%. At year 0 all the utilities do not have renewables at all and their renewable penetration start to increase year by year. By year 5, the group-1 utilities have 25% renewable penetration and group-2 utilities have 50% renewable penetration. In the second scenario, group-1 utilities do not increase their renewable penetration, while group-2 utilities have an annual increase at 10%.

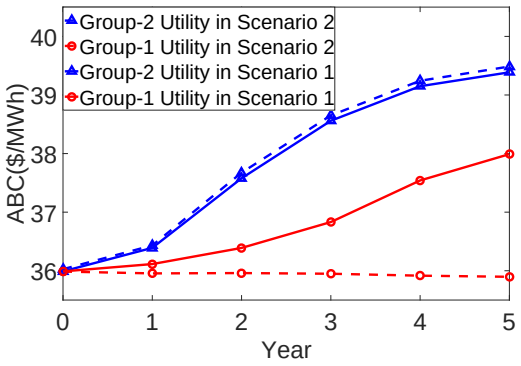

Fig. 9. The mean of ABC for different groups of utilities.

Observations: Fig. 9 shows the mean of ABC for the two groups of utilities in different scenarios. In the first scenario (shown in solid line), we can observe that as renewable penetration increases year by year, all the utilities in the market suffer an increasing ABC. In particular, the utilities with higher renewable penetration have higher ABCs. This result depicts the significance of the local impact. In the second scenario (shown in dash line), we can observe that the ABC of group-1 utilities decrease slightly, which demonstrates the existence of global impact from the group-2 utilities. In addition, we note that the ABC of group-2 utilities in scenario 1 is slightly smaller than that in scenario 2. This is because in scenario 1 the renewable penetration in group-1 utilities also increase and they have global impact on the group-2 utilities.

V. Conclusion

In this paper, we investigated the impact of the uncertainty from distributed renewable sources in active districts on the efficiency of the deregulated electricity supply chain. Our comprehensive study demonstrated that the distribted renewable uncertainty can lead to (i) an increase in the average buying cost per unit electricity of the utility serving the active district, termed as local impact, and (ii) a decrease in the average buying cost per unit electricity of other utilities in the same regional market, termed as global impact. Putting together, these observations revealed the potential inefficiency in the operation of the current deregulated electricity market that was designed for the cases with low uncertainty in both supply and demand. An interesting future direction is then to investigate how to redesign the market operation to be robust against this demand side uncertainty.

[3]We note that when all the utilities increase the renewable penetration, the total demand will decrease and it may lead to a lower day-ahead price, which will decrease their ABC. In this paper, we do not consider this case and assume that the day-ahead price is not affected by the decreasing demand.

Appendix A
Proof Sketch of Lemma 1

Proof: Recall from (1) that the actual demand D_i for a particular hour of utility i is settled in two timescales: (i) an amount of $D_i - \Delta_i$ is settled in day-ahead operation at price p_d, and (ii) the remaining amount Δ_i is settled in real-time operation at the spot price p_s expressed in (3). Since Δ_i takes symmetric values in $\phi(\delta_i, \sigma^2_{-i})$, summing over these two cases will result in a fixed day-ahead market settlement p_d. Thus, the increase in δ_i will only affect the real-time settlement.

- When $\Delta_i = \delta_i > 0$, the total mismatch Δ follows $\mathcal{N}\left(\delta_i, \sigma^2_{-i}\right)$ where the variance σ^2_{-i} is fixed under the setting of Lemma 1. For large $\delta_i > 0$, Δ tends to take large positive values. As spot price p_s is increasing w.r.t. Δ, large positive Δ leads to large positive p_s (and indeed large positive $p_s - p_d$ according to (3)). Thus, in real-time operation, the utility i will buy electricity at a statistically high price to settle the positive mismatch δ_i.
- When Δ_i takes the symmetric value $-\delta_i < 0$ (of the same magnitude), the total mismatch $\Delta \sim \mathcal{N}\left(-\delta_i, \sigma^2_{-i}\right)$. Following similar arguments, the utility i will sell at statistically low spot price to settle the negative mismatch.

In the first case, utility i will buy δ_i amount of electricity at a price that is higher than p_d and proportional to δ_i, denoted as p_{s1}. In the second case, it will sell δ_i amount of electricity at a price that is lower than p_d and proportional to $(-\delta_i)$, denoted as p_{s2}. Hence, the real-time settlement cost of utility i, summing over these two equally-likely cases, i.e., $\delta_i(p_{s1} - p_{s2})$ is positive and increasing w.r.t. δ_i, and thus $\phi(\delta_i, \sigma^2_{-i})$ increases as (the magnitude) δ_i increases. ■

Appendix B
Proof Sketch of Lemma 2

Proof: Following similar arguments in the proof sketch of Lemma 1, we know that σ^2_{-i} affects $\phi(\delta_i, \sigma^2_{-i})$ only through the real-time settlement. Meanwhile, when $\Delta_i = \delta_i > 0$ is fixed[4], the total imbalance Δ follows a normal distribution with mean δ_i and variance σ^2_{-i}. Let's begin with the following two simple cases to see the intuition:

- If $a_1 = a_2$, $b_1 = b_2$ in the pricing model, then the spot price p_s is a linear continuous function in Δ. Fig. 10 shows the spot price function and the distribution of Δ. We can observe that the real-time settlement cost on average is invariant to the changes in σ^2_{-i}, due to the symmetry property in the distribution of Δ.
- If $a_1 = a_2$, $b_1 > b_2$ in the pricing model, then the spot price p_s is a linear "step" function in Δ, as shown in Fig. 11. Unlike the first case, when $\Delta < 0$, the utility

[4]Similar arguments can be applied when $\Delta_i = -\delta_i < 0$.

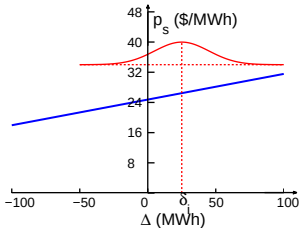

Fig. 10. Case 1: $a_1 = a_2$, $b_1 = b_2$.

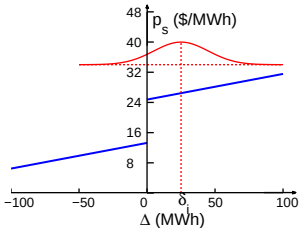

Fig. 11. Case 2: $a_1 = a_2$, $b_1 > b_2$.

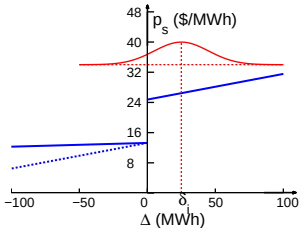

Fig. 12. $\Delta_i = \delta_i > 0$.

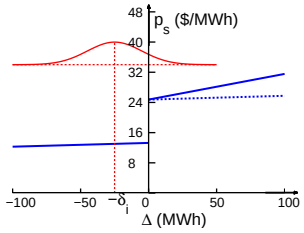

Fig. 13. $\Delta_i = -\delta_i < 0$.

can buy electricity at a spot price that is much lower, indicating a gain for the utility. In other words, as long as the sign of Δ is different from that of Δ_i, utility i will gain from the market. Increasing σ_{-i}^2 in this case will increase the probability of utility i to gain, thus its real-time settlement cost will decrease.

In Lemma 2, we consider the pricing model in (3), where $a_1 > a_2, b_1 > b_2$. For ease of discussion, let's denote the slope of the spot price function as k_1 when $\Delta > 0$ and k_2 when $\Delta < 0$, respectively. Thus $k_1 = a_1 > k_2 = a_2$. In this case, summing the real-time settlement cost over two equally-likely cases, i.e., $\Delta_i = \delta_i > 0$ and $\Delta_i = -\delta_i < 0$, can be shown to be the same as the case when summing over $\Delta_i = \delta_i > 0$ and $\Delta_i = -\delta_i < 0$ under the setting where $k_1 = k_2$. To see this, let's consider the following two cases:

- As shown in Fig. 12, if $\Delta_i = \delta_i > 0$, when $\Delta = -\delta < 0$, the real-time settlement cost for utility i will increase by $(a_1 - a_2)\delta$ as compared to the case when $k_1 = k_2 = a_1$.
- As shown in Fig. 13, if $\Delta_i = -\delta_i < 0$, when $\Delta = \delta > 0$, the real-time settlement cost for utility i will decrease by $(a_1 - a_2)\delta$ as compared to the case when $k_1 = k_2 = a_2$.

Now summing over these two cases results in a real-time settlement cost that is the same as that of summing over these two cases under the setting where $k_1 = k_2$. As discussed before, when $k_1 = k_2$, increasing σ_{-i}^2 will decrease real-time settlement cost. Consequently $\phi(\delta_i, \sigma_{-i}^2)$ is decreasing w.r.t. σ_{-i}^2. ■

Appendix C
Intuitive Explanation for Global Impact

In this appendix, we present the intuitive explanation for the global impact, i.e., fixed σ_i^2, $\mathbb{E}[\mathsf{ABC}_i]$ decreases w.r.t. σ_{-i}^2. According to the independent assumption of Δ_i and Δ_{-i}, the $\mathbb{E}[\mathsf{ABC}_i]$ can be expressed as:

$$\mathbb{E}[\mathsf{ABC}_i] = \int_0^\infty \int_0^\infty \omega(\delta_i, \delta_{-i}) f_{\Delta_i}(\delta_i) f_{\Delta_{-i}}(\delta_{-i}) d\delta_i d\delta_{-i},$$

where

$$\begin{aligned}\omega(\delta_i, \delta_{-i}) =& \mathbb{E}[\mathsf{ABC}_i | \Delta_i = \delta_i, \Delta_{-i} = \delta_{-i}] \\ &+ \mathbb{E}[\mathsf{ABC}_i | \Delta_i = \delta_i, \Delta_{-i} = -\delta_{-i}] \\ &+ \mathbb{E}[\mathsf{ABC}_i | \Delta_i = -\delta_i, \Delta_{-i} = \delta_{-i}] \\ &+ \mathbb{E}[\mathsf{ABC}_i | \Delta_i = -\delta_i, \Delta_{-i} = -\delta_{-i}],\end{aligned}$$

$\delta_i, \delta_{-i} > 0$ and $f_{\Delta_i}(\cdot)$ and $f_{\Delta_{-i}}(\cdot)$ are the PDF of random variable Δ_i and Δ_{-i}, respectively. Since $\delta_i + \delta_{-i} > 0$, $-(\delta_i + \delta_{-i}) < 0$, we have

$$\begin{aligned}&\mathbb{E}[\mathsf{ABC}_i | \Delta_i = \delta_i, \Delta_{-i} = \delta_{-i}] \\ &= \frac{p_d}{D_i}(D_i - \delta_i) + \frac{p_d \delta_i}{D_i}(a_1\delta_i + a_1\delta_{-i} + b_1),\end{aligned}$$

$$\begin{aligned}&\mathbb{E}[\mathsf{ABC}_i | \Delta_i = -\delta_i, \Delta_{-i} = -\delta_{-i}] \\ &= \frac{p_d}{D_i}(D_i + \delta_i) + \frac{p_d \delta_i}{D_i}(a_2\delta_i + a_2\delta_{-i} - b_2).\end{aligned}$$

If $\delta_{-i} < \delta_i$, we have

$$\begin{aligned}&\mathbb{E}[\mathsf{ABC}_i | \Delta_i = \delta_i, \Delta_{-i} = -\delta_{-i}] \\ &= \frac{p_d}{D_i}(D_i - \delta_i) + \frac{p_d \delta_i}{D_i}(a_1\delta_i - a_1\delta_{-i} + b_1),\end{aligned}$$

$$\begin{aligned}&\mathbb{E}[\mathsf{ABC}_i | \Delta_i = -\delta_i, \Delta_{-i} = \delta_{-i}] \\ &= \frac{p_d}{D_i}(D_i + \delta_i) + \frac{p_d \delta_i}{D_i}(-a_2\delta_i + a_2\delta_{-i} + b_2).\end{aligned}$$

Summing the above four terms we have for $\delta_{-i} < \delta_i$,

$$\omega(\delta_i, \delta_{-i}) = 4p_d + \frac{2p_d\delta_i}{D_i}((a_1 + a_2)\delta_i + b_1 - b_2). \quad (10)$$

Similarly, when $\delta_{-i} > \delta_i$, following similar calculation we have

$$\omega(\delta_i, \delta_{-i}) = 4p_d + \frac{2p_d\delta_i}{D_i}(a_1 + a_2)\delta_i. \quad (11)$$

Now we can observe that fixed δ_i, when δ_{-i} increases, if it is always less (or larger) than δ_i, from (10) (or (11)) we know that the $\omega(\delta_i, \delta_{-i})$ remains unchanged. If δ_{-i} increases from $\delta_{-i} < \delta_i$ to $\delta_{-i} > \delta_i$, the $\omega(\delta_i, \delta_{-i})$ decreases due to the positive term $b_1 - b_2$. Thus $\omega(\delta_i, \delta_{-i})$ is non-increasing w.r.t. δ_{-i}. Note that in this case, the gap $(b_1 - b_2)$ at $\Delta = 0$ in the pricing model in (3) is the key factor that cause the ABC_i to decrease.

Finally, we note that as σ_{-i}^2 increases, the random variable Δ_{-i} is more likely to take value of large magnitude, resulting in a large δ_{-i}. Thus given fixed σ_i^2, $\mathbb{E}[\mathsf{ABC}_i]$ decreases as σ_{-i}^2 increases.

References

[1] ISO New England. Internet: http://www.iso-ne.com/.
[2] Nord Pool. Internet: http://www.nordpoolspot.com/How-does-it-work/.
[3] NYISO Market. Internet: http://www.nyiso.com/public/media_room/publications_presentations/index.jsp.
[4] Pennsylvania State Climatologist. Internet: http://climate.psu.edu/data/.
[5] PJM. Internet: http://pjm.com/markets-and-operations/energy.aspx.

[6] E. Y. Bitar, R. Rajagopal, P. P. Khargonekar, K. Poolla, and P. Varaiya, "Bringing wind energy to market," *IEEE Trans. Power Syst.*, vol. 27, no. 3, pp. 1225–1235, 2012.

[7] H. Bludszuweit, J. A. Domínguez-Navarro, and A. Llombart, "Statistical analysis of wind power forecast error," *IEEE Trans. Power Syst.*, vol. 23, no. 3, pp. 983–991, 2008.

[8] D. W. Cai, S. Adlakha, S. H. Low, P. De Martini, and K. M. Chandy, "Impact of residential pv adoption on retail electricity rates," *Energy Policy*, vol. 62, pp. 830–843, 2013.

[9] H. Demuth and M. Beale, "Neural network toolbox for use with matlab," 1993.

[10] S.-E. Fleten and E. Pettersen, "Constructing bidding curves for a price-taking retailer in the norwegian electricity market," *IEEE Trans. Power Syst.*, vol. 20, no. 2, pp. 701–708, 2005.

[11] M. H. Hajiesmaili, C.-K. Chau, M. Chen, and L. Huang, "Online microgrid energy generation scheduling revisited: The benefits of randomization and interval prediction," in *Proc. ACM e-Energy*, 2016.

[12] L. Jia and L. Tong, "Renewables and storage in distribution systems: Centralized vs. decentralized integration," *IEEE JSAC*, vol. 34, no. 3, pp. 665–674, 2016.

[13] D. Kirschen and G. Strbac, *Fundamentals of Power System Economics*. John Wiley & Sons, Ltd, 2004.

[14] L. Lu, J. Tu, C.-K. Chau, M. Chen, and X. Lin, "Online energy generation scheduling for microgrids with intermittent energy sources and co-generation," in *Proc. ACM SIGMETRICS*, vol. 41, 2013, pp. 53–66.

[15] C. Marnay and R. Firestone, "Microgrids: An emerging paradigm for meeting building electricity and heat requirements efficiently and with appropriate energy quality," *Lawrence Berkeley National Laboratory*, 2007.

[16] D. McConnell, P. Hearps, D. Eales, M. Sandiford, R. Dunn, M. Wright, and L. Bateman, "Retrospective modeling of the merit-order effect on wholesale electricity prices from distributed photovoltaic generation in the australian national electricity market," *Energy Policy*, vol. 58, pp. 17–27, 2013.

[17] J. Nair, S. Adlakha, and A. Wierman, "Energy procurement strategies in the presence of intermittent sources," in *Proc. ACM SIGMETRICS*, vol. 42, 2014, pp. 85–97.

[18] B. Neupane, T. B. Pedersen, and B. Thiesson, "Evaluating the value of flexibility in energy regulation markets," in *Proc. ACM e-Energy*, 2015, pp. 131–140.

[19] R. Rajagopal, E. Bitar, F. Wu, and P. Varaiya, "Risk limiting dispatch of wind power," in *IEEE ACC*, 2012, pp. 4417–4422.

[20] J. L. Sawin *et al.*, "Renewables 2015 global status report-annual reporting on renewables: Ten years of excellence," REN 21, Tech. Rep., 2015. [Online]. Available: http://www.ren21.net/wp-content/uploads/2015/07/REN12-GSR2015_Onlinebook_low1.pdf

[21] R. Sioshansi, "Evaluating the impacts of real-time pricing on the cost and value of wind generation," *IEEE Trans. Power Syst.*, vol. 25, no. 2, pp. 741–748, 2010.

[22] K. Skytte, "The regulating power market on the nordic power exchange nord pool: an econometric analysis," *Energy Economics*, vol. 21, no. 4, pp. 295–308, 1999.

[23] T. Wang, A. Atasu, and M. Kurtulus, "A multiordering newsvendor model with dynamic forecast evolution," *Manufacturing & Service Operations Management*, vol. 14, no. 3, pp. 472–484, 2012.

[24] H. Yi, M. H. Hajiesmaili, Y. Zhang, M. Chen, and X. Lin, "Impact of the uncertainty of distributed renewable generation on deregulated electricity supply chain," The Chinese University of Hong Kong, Tech. Rep., 2016. [Online]. Available: http://staff.ie.cuhk.edu.hk/~mhchen/papers/impact-of-renewables.pdf

[25] Y. Zhang, M. Hajiesmaili, S. Cai, M. Chen, and Q. Zhu, "Peak-aware online economic dispatching for microgrids," *IEEE Trans. Smart Grid*, 2016.

[26] M. Zugno, J. M. Morales, P. Pinson, and H. Madsen, "Pool strategy of a price-maker wind power producer," *IEEE Trans. Power Syst.*, vol. 28, no. 3, pp. 3440–3450, 2013.

Hanling Yi received his B.Eng. degree from the Department of Electronic Engineering and Information Science at University of Science and Technology of China, Hefei, China in 2014, and is currently pursuing the Ph.D. degree in Department of Information Engineering at the Chinese University of Hong Kong. His research interests include electricity market and microgrid operation.

Mohammad H. Hajiesmaili received the B.Sc. degree in Computer Engineering from the Department of Computer Engineering, Sharif University of Technology, Iran, in 2007, and the M.Sc. and Ph.D. degrees in Computer Engineering from the Electrical and Computer Engineering Department, University of Tehran, Iran, in 2009 and 2014, respectively. He was a Postdoctoral Fellow with the Department of Information Engineering, The Chinese University of Hong Kong, from 2014 to 2016. He is currently a Postdoctoral Fellow with the Department of Electrical and Computer Engineering, Johns Hopkins University. His research interests include optimization, algorithm, and mechanism design in communication, energy, and transportation networks.

Ying Zhang received his B.Eng. degree from the Department of Electronic Engineering at Shanghai Jiao Tong University in 2013, and is currenty pursuing the Ph.D. degree in Department of Information Engineering at the Chinese University of Hong Kong. His research interests include energy systems and distributed optimization. He is also interested in statistical arbitrage and high frequency trading.

Minghua Chen (S'04 M'06 SM'13) received his B.Eng. and M.S. degrees from the Dept. of Electronic Engineering at Tsinghua University in 1999 and 2001, respectively. He received his Ph.D. degree from the Dept. of Electrical Engineering and Computer Sciences at University of California at Berkeley in 2006. He spent one year visiting Microsoft Research Redmond as a Postdoc Researcher. He joined the Dept. of Information Engineering, the Chinese University of Hong Kong in 2007, where he is currently an Associate Professor. He is also an Adjunct Associate Professor in Institute of Interdisciplinary Information Sciences, Tsinghua University. He received the Eli Jury award from UC Berkeley in 2007 (presented to a graduate student or recent alumnus for outstanding achievement in the area of Systems, Communications, Control, or Signal Processing) and The Chinese University of Hong Kong Young Researcher Award in 2013. He also received several best paper awards, including the IEEE ICME Best Paper Award in 2009, the IEEE Transactions on Multimedia Prize Paper Award in 2009, and the ACM Multimedia Best Paper Award in 2012. He is currently an Associate Editor of the IEEE/ACM Transactions on Networking. He serves as TPC Co-Chair of ACM e-Energy 2016 and General Chair of ACM e-Energy 2017. His current research interests include energy systems (e.g., smart power grids and energy-efficient data centers), intelligent transportation system, online competitive optimization, distributed optimization, networking, and delay-constrained network coding.

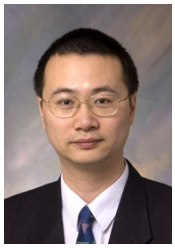

Xiaojun Lin (S'02 M'05 SM'12 F'17) received his B.S. from Zhongshan University, Guangzhou, China, in 1994, and his M.S. and Ph.D. degrees from Purdue University, West Lafayette, IN, in 2000 and 2005, respectively. He is currently an Associate Professor of Electrical and Computer Engineering at Purdue University.

Dr. Lin's research interests are in the analysis, control and optimization of large and complex networked systems, including both communication networks and power grid. He received the IEEE INFOCOM 2008 best paper and 2005 best paper of the year award from Journal of Communications and Networks. His paper was also one of two runner-up papers for the best-paper award at IEEE INFOCOM 2005. He received the NSF CAREER award in 2007. He was the Workshop co-chair for IEEE GLOBECOM 2007, the Panel co-chair for WICON 2008, the TPC co-chair for ACM MobiHoc 2009, and the Mini-Conference co-chair for IEEE INFOCOM 2012. He is currently serving as an Associate Editor for IEEE/ACM Transactions on Networking and an Area Editor for (Elsevier) Computer Networks Journal, and has served as a Guest Editor for (Elsevier) Ad Hoc Networks journal.